European Journal of Chemistry

View Journal Online
View Article Online

# Exploring the thermoluminescent characteristics of nano α-$Al_2O_3$: Influence of heating rate on glow peaks and activation energy

Sahib Mammadov *, Muslim Gurbanov, and Ahmad Ahadov

*Institute of Radiation Problems, Ministry of Science and Education, 9, B. Vahabzade Str., Baku, 1143, Azerbaijan*

** Corresponding author at: Institute of Radiation Problems, Ministry of Science and Education, 9, B. Vahabzade Str., Baku, 1143, Azerbaijan.*
*e-mail: s.mammadov@irp.science.az (S. Mammadov).*

RESEARCH ARTICLE

10.5155/eurjchem.15.2.149-154.2552

Received: 21 March 2024
Received in revised form: 14 April 2024
Accepted: 4 May 2024
Published online: 30 June 2024
Printed: 30 June 2024

KEYWORDS

TL glow curve
Frequency factor
Nano alpha-$Al_2O_3$
Activation energy
Thermoluminescence
Variable heating rate method

ABSTRACT

The thermoluminescence (TL) characteristics of nano α-$Al_2O_3$ (40 nm) under varying heating rates have been investigated. The presented data reveal a significant displacement of glow peaks to higher temperatures as the heating rate increases, accompanied by variations in the height of the TL peaks. When the glow curve plot represents the TL intensity in counts/K against temperature (K), there is a noticeable shift towards higher temperatures with increasing heating rate. The activation energy ($E$) calculated using the two different heating rate methods is 1.08±0.7 eV. The $\ln(T^2_M/\beta)$ graph *versus* $1/kT_M$ yields an activation energy value of $E$ = 1.15±0.1 eV. This result agrees with data from the existing literature supporting the observed thermoluminescent behaviour of nano α-$Al_2O_3$ (40 nm) at different heating rates. The TL response and luminescence efficiency are examined in relation to changes in heating rate, revealing insights into thermal quenching phenomena. Additionally, activation energy calculations based on different heating rates are explored to understand the underlying mechanisms influencing TL behavior.

**Cite this**: *Eur. J. Chem.* **2024**, *15(2)*, 149-154 **Journal website**: www.eurjchem.com

## 1. Introduction

The dependence of the temperature at the peak maximum, $T_{max}$, of a thermoluminescence (TL) glow peak on the heating rate (for both first- and second-order kinetics) stands as a feature among the most well known in the literature of TL and corresponding applications [1,2]. The effect of the $T_{max}$ shift as a function of the heating rate makes the latter experimental parameter a very dynamic experimental tool. When the linear heating rate β changes, the temperature $T_M$ of the maximum TL intensity of the peak also changes: faster heating rates produce a temperature shift towards higher values of $T_{max}$. The widespread use of various heating rate analyses [3-5] often achieves detection of the depth and frequency factor of the trap. It must be emphasized that when the variable heating rate method of analysis is applied, good thermal contact between the heating element in the TL apparatus and the sample is essential.

Thermoluminescence nanodosimeters are commonly utilized in diverse applications, such as personal and environmental monitoring and clinical dosimetry [6]. Analyzing the glow curve and assessing trap parameters becomes essential for comprehending the behavior of TL materials. Luminescent materials have widespread applications in ionizing radiation dosimetry. Among these materials, aluminium oxide ($Al_2O_3$) sensitized with various dopants has been identified as a potential thermoluminescence dosimeter [7-10]. A comprehensive analysis of electron and hole traps is also significant when using aluminium nanooxides as catalysts or composite materials. The thermoluminescence response of gamma-irradiated nano-alumina, particularly the linearity of the dose-dependent response and its dependence on particle size, is reported elsewhere [7]. This study investigates the essential TL characteristics of nanoalumina as a potential matrix to develop doped dosimeters for ionizing radiation. The primary focus of this study is the parameters of the TL response of gamma-irradiated nanoalumina, particularly the dependence of the temperature at the peak maximum, $T_{max}$, of a TL glow peak on the heating rate.

## 2. Experimental

This study used nanosized α-$Al_2O_3$ particles with a size of 40 nm α-$Al_2O_3$ commercially available from Skyspring Nanomaterials, Inc. as samples. To obtain a good X-ray diffraction pattern, particle size characterization was carried out on the corundum (Figure 1). The measurements of the X-ray diffraction were carried out at ambient temperature. PXRD was performed using a D2Phaser (Bruker) diffractometer with Ni-filtered CuKα radiation (λ = 1.54060 Å) on randomly oriented samples.


ISSN 2153-2249 (Print) / ISSN 2153-2257 (Online) 
https://dx.doi.org/10.5155/eurjchem.15.2.149-154.2552

**Table 1.** Basic parameters of the main glow peak of nano-α-alumina.

| Heat rate, °C/sec | $T_M$, °C | Area, a.u. | Full-width at half-maximum (FWHM) | Left half width | Right half width | $I_{max}$, a.u. |
|---|---|---|---|---|---|---|
| 2 | 184 | 51006 | 49.6 | 29.9 | 19.6 | 841 |
| 4 | 196 | 45597 | 49.3 | 29.7 | 19.7 | 793 |
| 6 | 202 | 43837 | 58.8 | 32.9 | 25.9 | 667 |
| 8 | 206 | 42574 | 61.5 | 41.4 | 20.1 | 624 |
| 12 | 212 | 33985 | 52.4 | 28.9 | 23.5 | 565 |

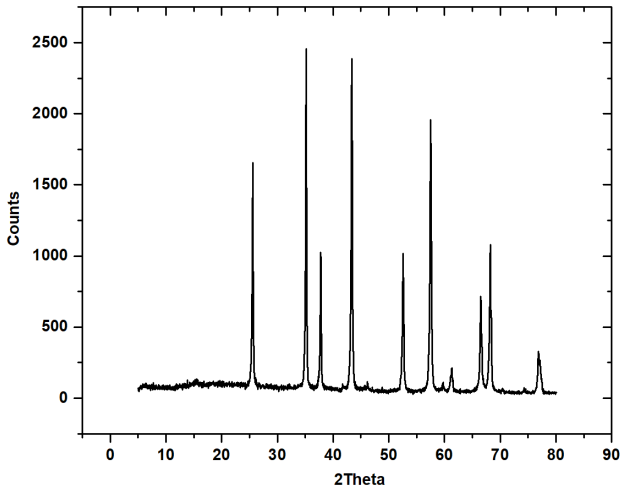


**Figure 1.** XRD pattern of nano α-alumina with the particle size of 40 nm.

The samples were scanned in the range 5 ≤ 2Θ ≤ 80° at a scan rate of 1.2 °/min. Semi-quantitative estimates of the abundance of mineral phases were derived from the PXRD data using the intensity of specific reflections, density, and mass absorption coefficients of the elements for CuKα radiation.

The samples were irradiated at room temperature with a $^{60}$Co-gamma source with a dose rate of 1.76 Gy/s. The dose rate was determined using a Magnette Miniscope MS400 EPR spectrometer with individually packed BioMax alanine dosimetry films with barcode markings developed by Eastman Kodak Company. The Harshaw TLD 3500 manual reader was used to assess the characteristics of TL samples using a different linear heating rate of 323 to 673 K in an $N_2$ atmosphere with a Pilkington HA-3 heat-absorbing filter. Three 5 mg aliquots each were used for each measurement, and the TL data points represented the average of the three aliquots. A thin layer of sample powder was evenly distributed on the planchet surface to ensure a uniform TL signal.

## 3. Results and discussion

A simple and practical way to understand the change in $T_{max}$ concerning $\beta$ is outlined below [2]. The likelihood of thermal stimulation is established during the thermoluminescence readout designed to record the TL peak. When the probability $p(t)$ of escaping electrons from the trap operates within a temperature range ΔT = 1 K, it depends on the heating rate. For example, with a heating rate of $\beta$ = 1 K/s, this duration is 1 second; at $\beta$ = 2 K/s, it is 0.5 seconds; and at $\beta$ = 5 K/s, it decreases to 0.2 seconds. In general, the time affecting ΔT = 1 K is given by $1/\beta$. Therefore, as the heating rate increases, the time allocated to each ΔT = 1 K decreases. This indicates that the number of trapped electrons thermally released within time intervals of $1/\beta$ per ΔT = 1 K is $\beta$ times less than that released in 1 second of $\beta$ = 1. The difference in thermally released electrons at ΔT = 1 K between the operating time of 1 second and $(1/\beta)$ seconds necessitates waiting for the temperature to rise before the thermal release occurs. This mechanism clarifies the shift of $T_{max}$ as a function of the heating rate. Various methods have been proposed to determine the activation energy through different heating rates [2,11]. The results from numerous TL phosphors indicate that calculating the integral of TL emission, the glow curve, using a temperature scale leads to a shift of the peak maximum temperature towards higher values. Moreover, there is a noticeable decrease in TL response in certain materials as the heating rate increases, a phenomenon attributed to thermal quenching.

The data illustrated in Figure 2 reveal that, as the heating rate increases, the glow peak shifts towards higher temperatures, accompanied by changes in the height of the thermoluminescence peak. When the linear heating rate $\beta$ changes, the temperature $T_M$ of the maximum TL intensity of the peak also changes: faster heating rates produce a temperature shift to higher $T_M$ values. This effect is shown in Figure 1. Since TL experiments typically involve collecting the TL signal over time, the $y$-axis in Figure 2 is expressed in counts per second. However, these counts/s units are unsuitable for graphing the actual TL glow curve, which is a function of temperature. To address this, each graph in Figure 2 is divided by the corresponding heating rate $\beta$ to convert the $y$-axis into counts per kelvin, as depicted in Figure 3. Table 1 summarizes the parameters of the main peak described in Figures 2 and 3.

There are several methods to calculate the activation energy based on changes in the heating rate [12,13]. The approach to determining the activation energy ($E$) utilizing two distinct heating rates for a first-order peak involves applying the maximum condition equation expressed as:

$$E = k\frac{T_{M1}T_{M2}}{T_{M1}-T_{M2}}ln\left[\frac{\beta_1}{\beta_2}\left(\frac{T_{M2}}{T_{M1}}\right)^2\right] \quad (1)$$

where $k$: Bolzman constants, $T_{M1}$ and $T_{M2}$ are the temperature at maximum height, $\beta_1$ and $\beta_2$ are the corresponding heating rates.

When $T_M$ can be measured with an accuracy of 1 °C, this method yields $E$ with a precision of 5%. Table 1 provides details on temperatures $T_M$, representing the maximum TL intensity, and heating rates at 2, 4, 6, 8, and 12 °C, obtained from the nano α-$Al_2O_3$ (40 nm) curves.

**Table 2.** Calculated activation energy utilizing two distinct heating rates.

| $T_1$, °C | $T_2$, °C | $T_1$, K | $T_2$, K | *E*, eV | |
|---|---|---|---|---|---|
| 184 | 196 | 457 | 469 | 0.99 | 1.08±0.07 |
| 184 | 202 | 457 | 475 | 1.06 | |
| 184 | 206 | 457 | 479 | 1.11 | |
| 184 | 212 | 457 | 485 | 1.14 | |

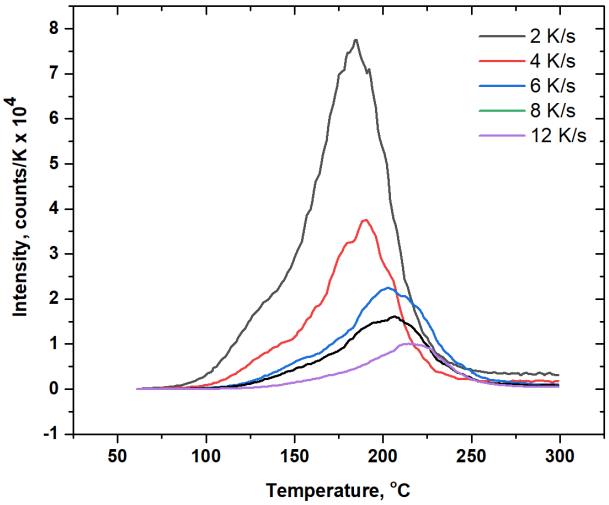


**Figure 2.** Experimental TL glow curve of nano-α-alumina at different heating rates. The *y*-axis represented in counts/K.

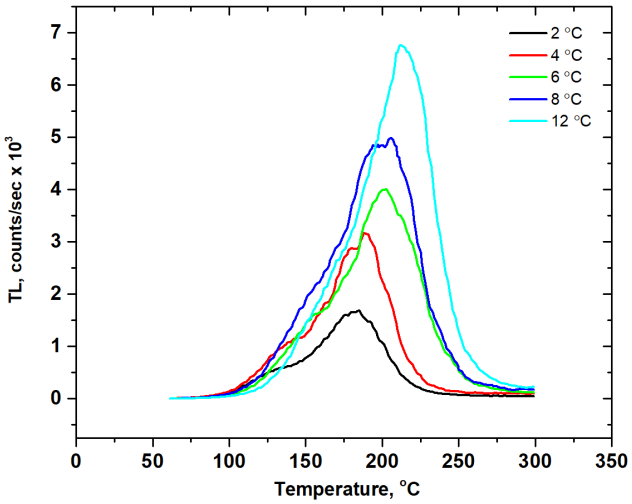


**Figure 3.** Experimental TL glow curve of nano-α-alumina at different heating rates. The *y-axis* is represented in counts/sec.

Table 2 summarizes the calculated activation energy values based on Equation 1. We derive the corresponding activation energy values by inserting $T_{M1}$, $T_{M2}$, $\beta_1$, and $\beta_2$ into Equation 1. The application of two different heating methods results in an average activation energy value of 1.08±0.07 eV.

Another approach by reference [13], based on the first-order equation, suggests employing multiple heating rates and results in the linear relation:

$$ln\left(\frac{T_M^2}{\beta}\right) = \frac{E}{kT_M} + ln\left(\frac{E}{sk}\right) \quad (2)$$

The resulting plot of $\ln(T^2_M/\beta$ versus $1/kT_M$ should produce a straight line with a slope of $E$ (activation energy) and an intercept of $\ln(E/sk)$. (s represents the frequency factor). Chen and Winer [14] demonstrated that when dealing with a temperature-dependent preexponential factor s (proportional to Tα), the plot of $\ln(T^2_M/\beta)$ against $1/kT_M$, it is expected to generate a linear relationship with a slope of $E + \alpha kT_M$, instead of the actual activation energy $E$. The energy $E$ can be calculated using the two-heating rate equation (Equation 2). The calculations involve determining the values of $1/kT_M$ (where k represents the Boltzmann constant) and ln $(T_M^2/\beta)$, as presented in Table 1, with $\beta$ denoting the specified heating rates. As explained above, Equation 2 establishes that the gradient of ln $(T_M^2/\beta)$ versus $1/kT_M$ graph is equivalent to the activation energy $E$, while the $y$-intercept corresponds to $\ln(E/sk)$ (Figure 4).

Using the slope and intercept obtained from the $\ln(T_M^2/\beta)$ *versus* $1/kT_M$ graph, one can subsequently derive the kinetic parameters $E$ and s as outlined. From the slope of the graph, $E$ = 1.15±0.1 eV. Using the value of the $y$-intercept = $\ln(E/sk)$, we obtain $s = E\times\exp(\text{intercept}/k) = 1.15\times\exp(17.57/8.617\times10^{-5}) = 5.70\times10^{11}\ s^{-1}$.

According to the one trap one recombination (OTOR) model of thermoluminescence, given that the test dose remains constant, the integral of the glow curve must remain stable and

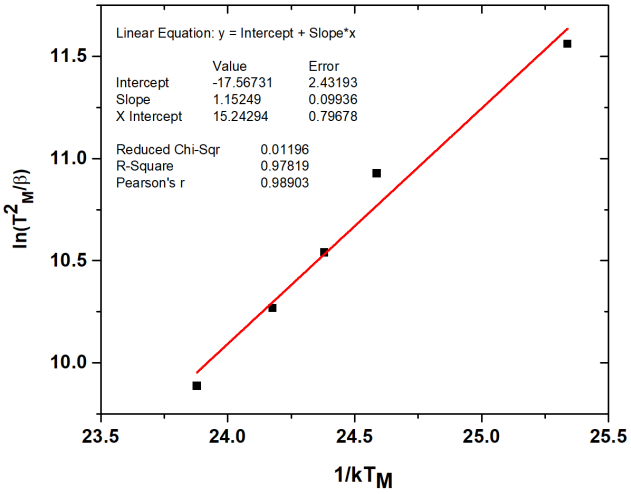


**Figure 4.** Graph of $\ln(T^2_M/\beta)$ versus $1/kT_M$ ($eV^{-1}$) to determine E and s.

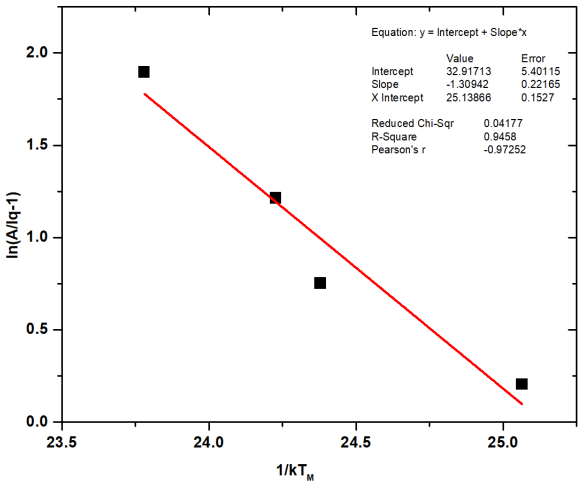


**Figure 5.** Evaluation of quenching parameters according to Equation 5.

unaffected by the heating rate. Therefore, for a consistent value of n0, there is no physical reason for the area to increase with increasing heating rate, as shown in Figure 1, or decrease with increasing heating rate, as depicted in Figure 2. The decrease in the peak area with an increase in the heating rate indicates that thermal quenching affects the glow peak [13]. The thermal quenching of luminescence efficiency is a phenomenon observed in many thermoluminescent materials [15], causing a significant reduction in the luminescence signal and altering the shape of the glow peaks. Among TL materials prone to thermal quenching, the most extensively studied include $Al_2O_3$:C [16] and Quartz [17]. The heating rate represents one of the most crucial experimental variables capable of altering the shape of the glow curve [18,19]. In thermoluminescence dosimetry, variations in heating rate can influence both the absorbed dose and the TL intensity [20,21]. The reduction in luminescence efficiency with increasing temperature, attributed to the increased probability of nonradiative transitions, is commonly referred to as thermal quenching [15]. As explained previously, the impact of thermal quenching becomes evident when conducting a series of TL measurements with different heating rates. Typically, as the heating rate increases, the peak of the TL glow shifts towards higher temperatures. At elevated temperatures, the luminescence is more intensely quenched, leading to a decrease in the overall area under the TL peak. The efficiency of thermal quenching with respect to temperature, denoted as η(T), is described by Equation 3 [17], where C and W represent the quenching parameters.

$$\eta(T) = \frac{I_q}{I_{uq}} = \frac{1}{1+Cexp(^{-W}/_{kT_M})} \quad (3)$$

where $I_q$ and $I_{uq}$ represent the area of the quenched and unquenched glow curve, C and W are the thermal quenching preexponential factor and activation energy, respectively [13].

In a series of glow curves recorded at various heating rates, it is assumed that the thermoluminescence measured at the lowest heating rate experiences the least amount of quenching. If we designate the area of the glow peak recorded at 2 °C/s as A, considered as unquenched, then the quenched TL intensity Iq can be expressed as Iq = Aη(T). Since TL peaks generally cover a narrow temperature range in practical scenarios, we can approximate the quenching function η(T) by its value at the maximum of the peak, denoted as $\eta(T_M)$. In this scenario, Equation 3 is reformulated as

$$I_q = \frac{A}{1+Cexp(^{-W}/_{kT_M})} \quad (4)$$

If rearranged, it can be written as

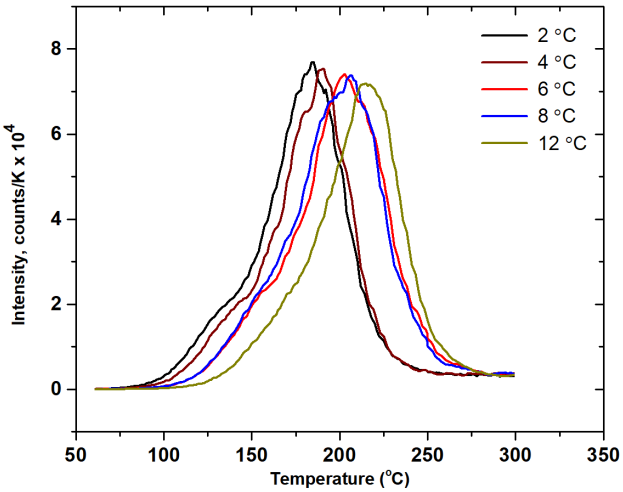


**Figure 6.** Unquenched glow curves (corrected) for heating rates 2, 4, 6, 8, and 12 °C.

$$\frac{A}{I_q} - 1 = Cexp\left(-W/kT_M\right) \quad (5)$$

Equation 5 indicates that plotting ln(A/Iq - 1) against $1/kT_M$ ($eV^{-1}$) will result in a straight line with a slope of -W and an intercept of ln(C), allowing for the evaluation of C. Details on implementing this method with the commercial dosimetric material TLD 500 can be found in the Reference [22].

Using the values of Iq and $T_{Mq}$ in Table 1, and assuming a constant peak integral A = 1,000, Figure 5 displays the graph of ln(A/Iq - 1) against $1/kT_M$. The quenching parameters derived from Figure 5 are W = 1.31 eV and C = $1.98\times10^{14}$ $s^{-1}$. Using these parameters and Equation 3, an unquenched glow curve has been calculated and Figure 6 represents the calculated glow curve for the corresponding heating rates.

The thermal quenching model, based on the Mott-Seitz mechanism presented in reference [23], elucidates the behavior of electrons within the traps responsible for the dosimetric peaks. According to this model, electrons within the trap are stimulated thermally (via heating) to rise to the conduction band. Subsequently, these electrons transition from the conduction band to an excited recombination level. In the next stage, electrons in this excited state undergo recombination in two distinct manners: i) some electrons move to the ground level, recombine, and emit light; ii) others undergo a non-radiative process that competes thermally with the recombination at the ground level of the center. As the sample temperature increases, more electrons are diverted from the excited state via nonradiative pathways. This reduction in available electrons correlates with a decrease in the intensity of the luminescence signal.

## 4. Conclusions

Analysis of the thermoluminescence behavior of nano α-$Al_2O_3$ (40 nm) at various heating rates reveals that as the heating rate increases, the glow peak shifts toward higher temperatures, accompanied by alterations in the height of the TL peak. Using the two-heating rate equation, the activation energy *E* is determined as *E* = 1.08±0.07 eV. The analysis of the ln ($T_M^2/\beta$) versus $1/kT_M$ graph yields an activation energy of *E* = 1.15±0.1 eV. The frequency factor s has been estimated as s = $5.70\times10^{11}$ $s^{-1}$ but it is potentially affected by thermal quenching. The observed decrease in the TL intensity with the rising temperature reflects thermal quenching effects, elucidating the challenges in maintaining luminescence efficiency under varying experimental conditions. These findings contribute to advancing our understanding of TL dosimetry and underscore the importance of considering the heating rate as a critical experimental variable in TL studies. The main dosimetric peak at approximately 460 K is inherent to nano α-alumina alone, while different dopants are accountable for shifting the peak's maximum temperature ($T_M$) and potentially influencing its sensitivity.

## Acknowledgements

We thank anonymous reviewers for their constructive comments. The authors especially thank Prof. Amiraslanov Imadeddin from the Institute of Physics, Ministry of Education and Science of the Azerbaijan Republic for his support and technical cooperation.

## Disclosure statement

Conflict of interest: The authors declare that they have no conflict of interest. Ethical approval: All ethical guidelines have been adhered to.

## CRediT authorship contribution statement

Conceptualization: Sahib Mammadov; Methodology: Ahamad Ahadov Software: Ahmad Ahadov; Validation: Muslim Gurbanov; Formal Analysis: Sahib Mammadov Investigation: Ahmad Ahadov; Resources: Muslim Gurbanov; Data Curation: Sahib Mammadov; Writing - Original Draft: Sahib Mammadov; Writing - Review and Editing: Sahib Mammadov, Muslim Gurbanov; Visualization: Ahmad Ahadov; Supervision: Muslim Gurbanov.

## ORCID and Email

Sahib Mammadov
s.mammadov@irp.science.az
mammadov_sahib@yahoo.com
https://orcid.org/0000-0002-4547-4491
Muslim Gurbanov
mgurbanov51@gmail.com
https://orcid.org/0000-0003-3321-1026
Ahmad Ahadov
a.ahadov@irp.science.az
https://orcid.org/0000-0002-6039-8714

## References

[1]. Furetta, C.; Kitis, G. Models in thermoluminescence. *J. Mater. Sci.* **2004**, *39*, 2277–2294.
[2]. Kitis, G.; Mouza, E.; Polymeris, G. S. The shift of the thermoluminescence peak maximum temperature versus heating rate, trap filling and trap emptying: Predictions, experimental

verification and comparison. *Physica B Condens. Matter* **2020**, *577*, 411754.
[3]. Rasheedy, M. S.; Zahran, E. M. The effect of the heating rate on the characteristics of some experimental thermoluminescence glow curves. *Phys. Scr.* **2006**, *73*, 98–102.
[4]. Rasheedy, M. S. A new evaluation technique for analyzing the thermoluminescence glow curve and calculating the trap parameters. *Thermochim. Acta* **2005**, *429*, 143–147.
[5]. Rasheedy, M. S. An independent method for obtaining the activation energy of thermoluminescence glow peaks. *Int. J. Mod. Phys. B* **2004**, *18*, 2877–2885.
[6]. Salah, A.; Farouk, S.; Ahmed, M.; El-Faramawy, N. Synthesis and thermoluminescence characteristics of beta irradiated nanocrystalline calcium aluminate doped with lanthanum oxides. *Radiat. Phys. Chem. Oxf. Engl. 1993* **2024**, *218*, 111571.
[7]. Mammadov, S.; Gurbanov, M.; Ahmadzade, L.; Abishov, A. Thermoluminescence properties of nano-alumina with two different particle sizes. *Phys. Chem. Solid State* (*Фізика і хімія твердого тіла*) **2023**, *24*, 584–588.
[8]. Binti Saharin, N. S.; Ahmad, N. E.; Tajuddin, H. A.; Tamuri, A. R. Thermoluminescence Properties of Aluminium Oxide doped Strontium, Lithium and Germanium prepared by Combustion Synthesis method. *EPJ Web Conf.* **2017**, *156*, 00001, https://doi.org/10.1051/epjconf/201715600001.
[9]. Salah, N.; Khan, Z. H.; Habib, S. S. Nanoparticles of Al2O3:Cr as a sensitive thermoluminescent material for high exposures of gamma rays irradiations. *Nucl. Instrum. Methods Phys. Res. B* **2011**, *269*, 401–404.
[10]. Salah, N. Nanocrystalline materials for the dosimetry of heavy charged particles: A review. *Radiat. Phys. Chem. Oxf. Engl. 1993* **2011**, *80*, 1–10.
[11]. Sadek, A. M.; Kitis, G. A critical look at the kinetic parameter values used in simulating the thermoluminescence glow-curve. *J. Lumin.* **2017**, *183*, 533–541.
[12]. Furetta, C. *Handbook of Thermoluminescence (2nd Edition)*; World Scientific Publishing: Singapore, Singapore, 2010.
[13]. Pagonis, V.; Kitis, G.; Furetta, C. *Numerical and Practical Exercises in Thermoluminescence*; Springer New York: New York, NY, 2006.
[14]. Chen, R. Methods for kinetic analysis of thermally stimulated processes. *J. Mater. Sci.* **1976**, *11*, 1521–1541.
[15]. Kadari, A.; Kadri, D. New numerical model for thermal quenching mechanism in quartz based on two-stage thermal stimulation of thermoluminescence model. *Arab. J. Chem.* **2015**, *8*, 798–802.
[16]. Chithambo, M. L. A method for kinetic analysis and study of thermal quenching in thermoluminescence based on use of the area under an isothermal decay-curve. *J. Lumin.* **2014**, *151*, 235–243.
[17]. Dawam, R. R.; Chithambo, M. L. Thermoluminescence of annealed synthetic quartz: The influence of annealing on kinetic parameters and thermal quenching. *Radiat. Meas.* **2018**, *120*, 47–52.
[18]. Chithambo, M. L.; Seneza, C.; Ogundare, F. O. Kinetic analysis of high temperature secondary thermoluminescence glow peaks in α-Al2O3:C. *Radiat. Meas.* **2014**, *66*, 21–30.
[19]. Subedi, B.; Kitis, G.; Pagonis, V. Simulation of the influence of thermal quenching on thermoluminescence glow-peaks. *Phys. Status Solidi (A)* **2010**, *207*, 1216–1226.
[20]. Kalita, J. M.; Wary, G. Kinetic analysis of thermoluminescence glow curve of Indian sillimanite. *Adv. Sci. Lett.* **2016**, *22*, 3854–3856.
[21]. Kalita, J. M.; Chithambo, M. L. Thermoluminescence of α-Al2O3:C,Mg: Kinetic analysis of the main glow peak. *J. Lumin.* **2017**, *182*, 177–182.
[22]. Akselrod, M. S.; Agersnap Larsen, N.; Whitley, V.; McKeever, S. W. S. Thermal quenching of *F*-center luminescence in Al2O3:C. *J. Appl. Phys.* **1998**, *84*, 3364–3373.
[23]. Pagonis, V.; Ankjærgaard, C.; Murray, A. S.; Jain, M.; Chen, R.; Lawless, J.; Greilich, S. Modelling the thermal quenching mechanism in quartz based on time-resolved optically stimulated luminescence. *J. Lumin.* **2010**, *130*, 902–909.